THE JOURNAL OF BIOLOGICAL CHEMISTRY VOL. 289, NO. 21, pp. 14731–14739, May 23, 2014

Mg^{2+}-dependent Interactions of ATP with the Cystathionine-β-Synthase (CBS) Domains of a Magnesium Transporter*

Received for publication, January 17, 2014, and in revised form, March 28, 2014 Published, JBC Papers in Press, April 6, 2014, DOI 10.1074/jbc.M114.551176

Yusuke Hirata[‡1], **Yosuke Funato**[‡], **Yu Takano**[§], **and Hiroaki Miki**[‡2]

From the [‡]*Department of Cellular Regulation, Research Institute for Microbial Diseases, Osaka University, Suita, Osaka 565-0871, Japan and the* [§]*Laboratory of Protein Informatics, Institute for Protein Research, Osaka University, Suita, Osaka 565-0871, Japan*

Background: CNNMs are evolutionarily conserved Mg^{2+} transporters that possess CBS domains.
Results: CBS domains are essential for molecular function, and they bind to ATP in a Mg^{2+}-dependent manner.
Conclusion: The unique binding feature with ATP may contribute to Mg^{2+} transport by CNNMs.
Significance: This is the first report showing the Mg^{2+}-dependent and specific interactions of ATP with CBS domains.

Ancient conserved domain protein/cyclin M (CNNM) family proteins are evolutionarily conserved Mg^{2+} transporters. However, their biochemical mechanism of action remains unknown. Here, we show the functional importance of the commonly conserved cystathionine-β-synthase (CBS) domains and reveal their unique binding ability to ATP. Deletion mutants of CNNM2 and CNNM4, lacking the CBS domains, are unable to promote Mg^{2+} efflux. Furthermore, the substitution of one amino acid residue in the CBS domains of CNNM2, which is associated with human hereditary hypomagnesemia, abrogates Mg^{2+} efflux. Binding analyses reveal that the CBS domains of CNNM2 bind directly to ATP and not AMP in a manner dependent on the presence of Mg^{2+}, which is inhibited in a similar pattern by the disease-associated amino acid substitution. The requirement of Mg^{2+} for these interactions is a unique feature among CBS domains, which can be explained by the presence of highly electronegative surface potentials around the ATP binding site on CNNM2. These results demonstrate that the CBS domains play essential roles in Mg^{2+} efflux, probably through interactions with ATP. Interactions with ATP, which mostly forms complexes with Mg^{2+} in cells, may account for the rapid Mg^{2+} transport by CNNM family proteins.

Magnesium is an essential element involved in a wide variety of biological activities. The homeostasis of magnesium levels is strictly regulated by intestinal absorption and renal reabsorption, in which the epithelia function as a barrier that permits selective and regulated transport of Mg^{2+} from apical to basolateral surfaces. Genomic analyses of familial cases of hypomagnesemia have identified key molecules directly involved in these processes (1, 2). One of the least characterized members among these is the ancient conserved domain protein/cyclin M (CNNM)[3] family.

CNNM family proteins commonly possess a domain that is highly conserved from bacteria to humans (3). In humans, the CNNM family consists of four members, CNNM1–4. These proteins show a multidomain structure, composed of a sequence motif present in the cyclin box, a cyclic nucleotide monophosphate binding domain, two tandem cystathionine-β-synthase (CBS) domains, and a DUF21 domain (3). Significant evidence has suggested the importance of CNNMs in Mg^{2+} transport (4–6). Our recent study revealed that CNNM4 localizes to the basolateral membrane of intestinal epithelial cells and extrudes intracellular Mg^{2+} to the outside of the cells in exchange for Na^+, thereby mediating the transcellular transport of Mg^{2+} through the epithelia (7). However, the functional importance of each domain or motif present in the CNNM family is poorly understood. The DUF21 and CBS domains are supposed to be important for the biological function, as stated by the studies on human hereditary diseases caused by mutations in the *CNNM* family gene. Several point mutations that cause Jalili syndrome, which is characterized by recessive amelogenesis imperfecta, occur in the DUF21 domain-encoding region in *CNNM4* (8, 9). In addition, a point mutation that causes familial dominant hypomagnesemia, a rare human disorder characterized by renal Mg^{2+} wasting, occurs in the CBS domain-encoding region in *CNNM2* (6).

CBS domains are small protein modules (typically 60 amino acid residues in length) that usually exist as two tandem repeats, each of which is made up of highly conserved two α-helices and three β-strands arranged in a β-α-β-β-α order (10). CBS domains were originally identified in human cystathionine-β-synthase (11) and subsequently found in thousands of cytosolic and membrane-associated proteins from all kingdoms of life (10). In addition to CNNMs, there is an example of a CBS domain-possessing Mg^{2+} transporter, and in the case of bacterial MgtE, the CBS domains are proposed to be important for the regulation of Mg^{2+} transporting activity (12, 13). The phys-

* This work was supported by Funding Program for Next Generation World-Leading Researchers from Japan Society for the Promotion of Science (JSPS) (to H. M.), Exciting Leading-Edge Research Projects from Osaka University (to H. M.), and Grants-in-aid for Scientific Research from JSPS and Ministry of Education, Culture, Sports, Science, and Technology-Japan (to H. M. and Y. F.).
[1] Supported by the Taniguchi Memorial Fellowship project funded by the Research Foundation for Microbial Diseases of Osaka University.
[2] To whom correspondence should be addressed: Dept. of Cellular Regulation, Research Institute for Microbial Diseases, Osaka University, 3-1 Yamadaoka, Suita, Osaka 565-0871, Japan. Tel.: 81-6-6879-8293; Fax: 81-6-6879-8295; E-mail: hmiki@biken.osaka-u.ac.jp.

[3] The abbreviations used are: CNNM, cyclin M; AMPK, AMP-activated protein kinase; CBS, cystathionine-β-synthase; ClC, chloride channel; IMPDH, inosine-5′-monophosphate dehydrogenase; PDB, Protein Data Bank; SPR, surface plasmon resonance.

iological importance of CBS domains has been demonstrated by a number of observations that point mutations found in several hereditary diseases occur in the CBS domain-encoding region in the genes and disrupt their protein functions (14). Recent studies have shown that adenine nucleotides, such as ATP, ADP, or AMP, can bind to CBS domains of several proteins, such as AMP-activated protein kinase (AMPK), inosine-5′-monophosphate dehydrogenase (IMPDH), and chloride channel (ClC) family proteins (10, 15). The functional consequences and physiological importance of interactions with adenine nucleotides have been characterized most extensively in the case of AMPK. The CBS domains of the regulatory γ-subunit of AMPK have two discrete sites that can bind to AMP, ADP, and ATP (named as site 1 and site 3) (16, 17). Structural and biochemical studies have shown that AMP or ADP binding, but not ATP binding, to site 3 promotes phosphorylation and inhibits the dephosphorylation of Thr-172 on the catalytic α-subunit, thereby maintaining AMPK in its most active form (17, 18). Phosphorylated AMPK is further activated by AMP binding, but not by either ADP or ATP binding, to site 1 (17, 18). Such intricate regulations of the activity are impaired by disease-associated amino acid substitutions found in patients with Wolff-Parkinson-White syndrome, indicating the physiological importance of interactions with adenine nucleotides (15, 17).

In this study, we examined the functional importance of the CBS domains of CNNM family proteins. Binding analyses revealed that the CBS domains of CNNM2 bind to ATP, but not AMP, in a manner dependent on the presence of Mg^{2+}. A mutation in the CBS domains of CNNM2 associated with hereditary hypomagnesemia and the equivalent mutation of CNNM4 completely abrogated their Mg^{2+} efflux functions. Furthermore, this mutation also abrogated the binding of the CBS domains of CNNM2 to ATP. These results demonstrate the crucial importance of the CBS domains for Mg^{2+} efflux function of CNNM family proteins probably via the interaction with ATP.

EXPERIMENTAL PROCEDURES

Materials—AMP sodium salt, ATP disodium salt hydrate, and the mouse and rabbit anti-FLAG antibodies were purchased from Sigma-Aldrich. [2,8-^{3}H]AMP (15 Ci/mmol) was purchased from Movarek, and [α-^{32}P]ATP (3000 Ci/mmol) was purchased from Izotop. Magnesium Green-AM and rhodamine-phalloidin were purchased from Invitrogen.

Constructs—cDNAs for mouse CNNM2 and human CNNM3 were obtained by performing PCR and verified by DNA sequencing. Human CNNM1 cDNA was purchased from Invitrogen (IMAGE: 40006972), and human CNNM4 cDNA was generated in a previous study (7). Amino acid-substituted mutants of mouse CNNM2 (T568I) and human CNNM4 (T495I) were generated using the QuikChange Site-directed Mutagenesis kit (Agilent). ΔCBS mutants of CNNM2(Δ469–578) and CNNM4(Δ396–505) deletion constructs were generated by ligating two PCR fragments. These cDNA fragments were inserted into pCMV-4A (Stratagene) for expression in mammalian culture cells. cDNAs for the CBS domains of human CNNM1(425–568), mouse CNNM2(442–579), human CNNM3(310–447), human CNNM4(359–511), and human IMPDH2(112–232) were obtained by PCR and verified by DNA sequencing. cDNA for the CBS domains of human ClC-5(568–746) was kindly provided by Dr. R. Dutzler (19). These cDNA fragments were inserted into pGEX-6p1 (GE Healthcare) for bacterial expression.

Cell Culture and Transfection—HEK293 cells were cultured in Dulbecco's modified Eagle's medium supplemented with 10% fetal bovine serum and antibiotics. Expression plasmids were transfected in each cell by using Lipofectamine 2000 (Invitrogen).

Mg^{2+} Imaging Analyses—Mg^{2+} imaging analyses with Magnesium Green were performed as described previously (7).

Preparation of Recombinant Proteins—Recombinant proteins of CBS domains of CNNM1–4, ClC-5, and IMPDH2 were expressed as GST fusion forms in *Escherichia coli* by using the expression constructs in pGEX-6p1 and were purified using glutathione-Sepharose beads (GE Healthcare). For surface plasmon resonance (SPR) analysis, the GST tag was cleaved off by digestion with PreScission protease (GE Healthcare).

SPR Analyses—The binding of Mg^{2+} and ATP to the CBS domains of CNNM2 was analyzed using Biacore T200 instrument with an S series CM5 sensor chip (GE Healthcare). GST-cleaved CBS-WT and CBS-T568I were immobilized onto the sensor chip by using a standard amine coupling protocol. Binding analyses were performed in running buffer (50 mM HEPES-KOH (pH 7.0), 140 mM KCl, 1 mM 2-mercaptoethanol, and 0.05% Tween 20) at 25 °C in the presence of 0, 0.5, or 10 mM $MgCl_2$. For analyses of Mg^{2+} binding, $MgCl_2$ was injected as an analyte in running buffer without $MgCl_2$. SPR data were analyzed using the Biacore T200 Evaluation software and fit to a 1:1 binding model using the following equation, $R = (R_{max} \times C)/(K_d + C)$, where R is the observed response, R_{max} is the maximal binding capacity, C is the analyte concentration, and K_d is the dissociation constant. For the injection of ATP with buffer switching, the dual injection mode was applied, according to the manufacturer's instructions. Observed responses were normalized to R_{max} for each experiment and are represented as normalized response unit (RU). For normalization of sensorgrams for ATP injection without significant responses, R_{max} of SPR responses to ATP injection in the presence of Mg^{2+} 10 mM from the CBS-WT surface was used.

Filter Binding Assays—Filter binding assays were performed in 10-μl reaction mixtures containing reaction buffer (50 mM HEPES-KOH (pH 7.0), 140 mM KCl, 1 mM 2-mercaptoethanol), 50 μM recombinant proteins, and various concentrations of [α-^{32}P]ATP (500 cpm/pmol) or [2,8-^{3}H]AMP (60 cpm/pmol) in the presence or absence of 10 mM $MgCl_2$. The reaction systems were incubated for 20 min at 25 °C and immediately filtered through nitrocellulose membranes (25-mm diameter, 0.22-μm pore size; Millipore), which were prewashed with reaction buffer and washed with 1 ml of ice-cold reaction buffer. Filters were dried, and the radioactivity was determined by scintillation counting using a LS-6500 scintillation counter (Beckman). Nonspecific binding was determined by control assays with GST and was subtracted. The data were analyzed using the GraphPad Prism software (version 4.0) and fit to a 1:1 binding model using the same equation used in SPR analyses,

where R was substituted with the amount of bound adenine nucleotides, C was substituted with the concentration of adenine nucleotides, and R_{max} was substituted with estimated maximum binding of adenine nucleotides. The data were normalized to the percentage of estimated maximum binding of ATP and are represented as the mean ± S.E. of three independent experiments. For competition assays, recombinant proteins were incubated with 5 μM [α-^{32}P]ATP (5000 cpm/pmol) and reaction buffer in the presence of increasing concentrations of ATP or AMP and were subsequently processed as described above.

Structural Analyses—Homology models for the CBS domains of CNNM1, CNNM2, and CNNM4 in complex with ATP were built using Spanner (20) based on the structures of the CBS domains of CorC (a bacterial homolog of CNNMs) from *Bordetella parapertussis* (Protein Data Bank (PDB) ID 3JTF), and that of IMPDH2 was built using Spanner based on the structure of and IMPDH from *Pseudomonas aeruginosa* (PDB ID 4DQW) (21). ATP was placed into the predicted binding sites, based on the similar structures in complex with ATP found from GIRAF (22). Electrostatic surface potentials were calculated for these modeled structures and the crystal structure of the CBS domains of human ClC-5 in complex with ATP (PDB ID 2J9L) (19) using the Adaptive Poisson-Boltzmann Solver software (23), mapped on the solvent-accessible surface, and visualized in PyMOL.

RESULTS

Indispensable Role of the CBS Domains in Mg^{2+} Efflux—In our previous study, we reported that CNNM4 can stimulate Mg^{2+} efflux when expressed in HEK293 cells (7). To examine whether the other CNNM family proteins also have the ability to stimulate Mg^{2+} efflux, we transfected HEK293 cells with CNNM1-FLAG, CNNM2-FLAG, CNNM3-FLAG, or CNNM4-FLAG (Fig. 1*A*, *lower panel*) and then, performed imaging analyses with Magnesium Green, a fluorescent indicator for Mg^{2+}. Cells were first loaded with Mg^{2+} by bathing them in a solution containing 40 mM Mg^{2+} and then exposed to a Mg^{2+}-free solution to promote Mg^{2+} efflux artificially. The intensity of fluorescent signals in the cells expressing CNNM4-FLAG rapidly decreased immediately after Mg^{2+} depletion, whereas only a very subtle decrease was observed in empty vector-transfected cells (Fig. 1*A*, *top*), thereby confirming our previous finding (7). A significant level of Mg^{2+} efflux was also observed in cells expressing CNNM2-FLAG. In contrast, only a very subtle level of Mg^{2+} efflux was observed in cells expressing CNNM1-FLAG, and no significant Mg^{2+} efflux was observed in the cells expressing CNNM3-FLAG. These data indicate that CNNM2 can also potently stimulate Mg^{2+} efflux, similar to the efflux induced by CNNM4, when expressed in HEK293 cells. To investigate the importance of the CBS domains of CNNM family proteins in their Mg^{2+} efflux functions, we constructed deletion mutants of CNNM2 and CNNM4 lacking CBS domains, called CNNM2-ΔCBS and CNNM4-ΔCBS, respectively. Similar Mg^{2+} imaging analyses showed that these ΔCBS mutants could not stimulate Mg^{2+} efflux (Fig. 1*B*). We performed confocal microscopy and confirmed that these ΔCBS mutants, like WT, were localized mostly to the plasma membrane (Fig. 1*C*). Collectively, these results indicate the importance of the CBS domains in Mg^{2+} efflux functions.

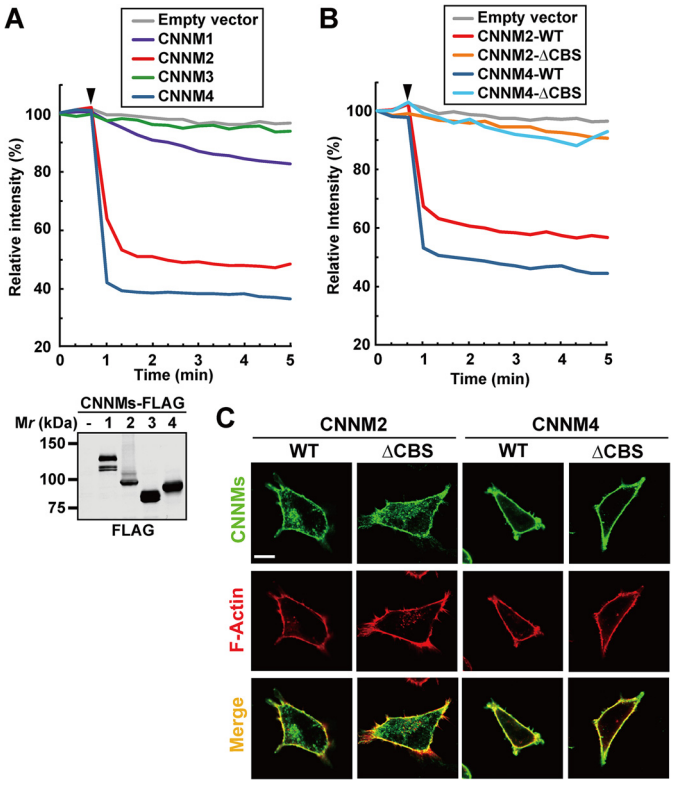

FIGURE 1. **Indispensable role of the CBS domains in Mg^{2+} efflux.** *A* and *B*, HEK293 cells transfected with the indicated constructs were subjected to Mg^{2+} efflux assays. The means of the relative fluorescence intensities of 10 cells are indicated. The *arrowheads* indicate the start point of Mg^{2+} depletion. The results of Western blotting analyses with the anti-FLAG antibody are also shown to indicate the similar level of expression for each CNNM isoform (*A*, *lower panel*). *C*, HEK293 cells transfected with the indicated constructs were subjected to immunostaining with anti-FLAG (*green*) and rhodamine-phalloidin (*red*) and were observed with a confocal microscope. *Scale bar*, 10 μm.

Disease-associated Amino Acid Substitution in the CBS Domains Completely Abrogates Mg^{2+} Efflux—Mutations in the *CNNM2* gene have recently been reported to be associated with human familial dominant hypomagnesemia (6). Two different mutations have been shown to occur in patients, and one of the mutations is an amino acid substitution of the threonine 568 residue with isoleucine, which is located in the CBS domains of CNNM2 (6). As shown in Fig. 2*A*, this threonine residue is completely conserved among CNNM family members across various species, ranging from bacteria to humans (indicated with the *asterisk*). To assess the importance of this mutation in the Mg^{2+} efflux function, we constructed the amino acid substitution mutants CNNM2-T568I and CNNM4-T495I, which is an equivalent mutant of CNNM4, and performed Mg^{2+}-imaging analyses with Magnesium Green, as described previously. Almost no Mg^{2+} efflux was observed in the cells expressing CNNM2-T568I or CNNM4-T495I (Fig. 2*B*). These mutant proteins, like WT proteins, were also localized mostly to the plasma membrane (Fig. 2*C*). These results confirm the importance of the highly conserved and disease-associated threonine residue in Mg^{2+} efflux functions, further supporting the role of the CBS domains.

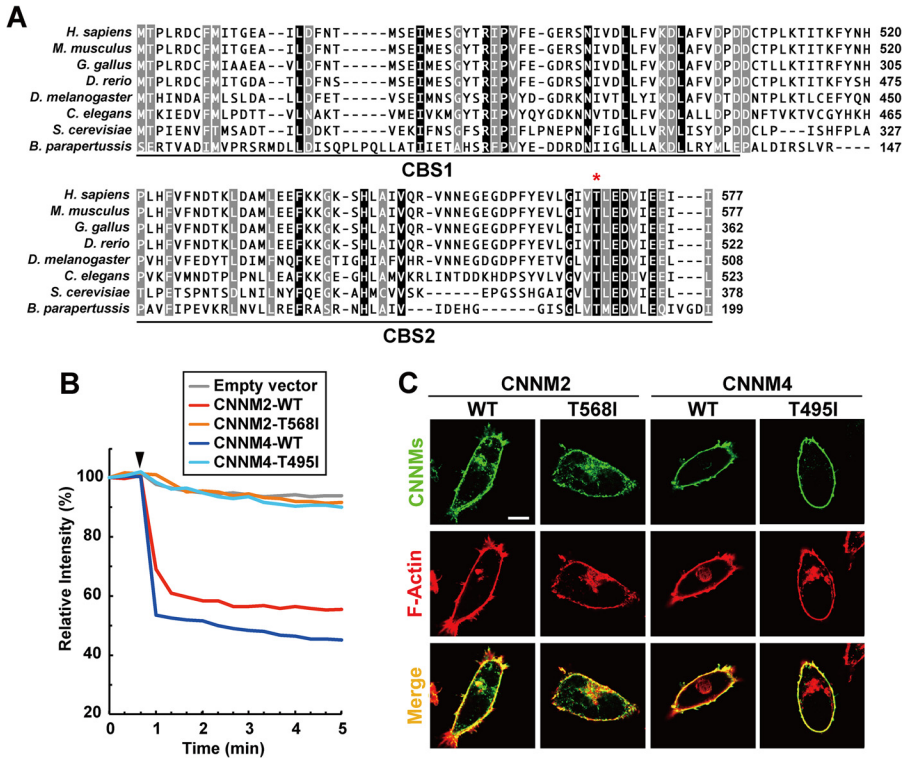

FIGURE 2. **Disease-associated amino acid substitution in the CBS domains abrogates Mg^{2+} efflux.** *A*, sequence alignment of two tandem CBS domains of CNNM family proteins from the following various species (NCBI protein database accession numbers are given in *parentheses*): *Homo sapiens* CNNM2 (NP_060119.3), *Mus musculus* CNNM2 (NP_291047.2), *Gallus gallus* CNNM2 (XP_426532.3), *Danio rerio* CNNM2 (NP_001138257.1), *Drosophila melanogaster* Unextended (ELP57407.1), *Caenorhabditis elegans* C52D10.12 (CAM36329.1), *Saccharomyces cerevisiae* Mam3p (EIW07873.1), and *Bordetella parapertussis* CorC (NP_883455.1). Identical residues in all of the species are *boxed in black*, and residues with one exception are *boxed in gray*. The *asterisk* indicates the conserved threonine residue, whose amino acid substitution in human CNNM2 is associated with familial dominant hypomagnesemia. *B*, HEK293 cells transfected with the indicated constructs were subjected to Mg^{2+} efflux assays. The means of relative fluorescence intensities of 10 cells are indicated. The *arrowhead* indicates the start point of Mg^{2+} depletion. *C*, HEK293 cells transfected with the indicated constructs were subjected to immunostaining with anti-FLAG (*green*) and rhodamine-phalloidin (*red*) and were observed using a confocal microscope. *Scale bar*, 10 μm.

ATP Binds to the CBS Domains of CNNM2 in a Mg^{2+}-dependent Manner—Adenine nucleotides have been shown to interact with the CBS domains of several proteins and to regulate their activities (10, 15). To investigate the possibility that adenine nucleotides can also interact with the CBS domains of CNNM family proteins, we performed binding analyses using SPR. Recombinant proteins of the CBS domains of wild-type CNNM2 (CBS-WT) were immobilized on the surface of a sensor chip, and various concentrations of ATP were injected over the SPR sensor surface as an analyte by using the running buffer that does not contain any divalent cation. However, no significant response was observed (data not shown). Because there are examples of proteins for which binding to ATP depends on the presence of Mg^{2+} (24–27), we determined to examine the interaction in the presence of Mg^{2+}. Before ATP binding analyses, we checked SPR responses using Mg^{2+} itself as an analyte. The results in Fig. 3*A* show a gradual and dose-dependent increase of responses, indicating the occurrence of direct interaction between Mg^{2+} and the CNNM2 CBS domains. However, this increase of the SPR response never reached plateau even at 10 mM, and thus, it was impossible to determine the K_d value for the interaction within the physiological range (0.5–1 mM). We then performed SPR analyses to examine the interaction of CBS-WT with ATP by setting the concentrations of Mg^{2+} to 0.5 mM and 10 mM. As shown in Fig. 3*B*, significant and dose-dependent SPR responses were observed, and the levels of

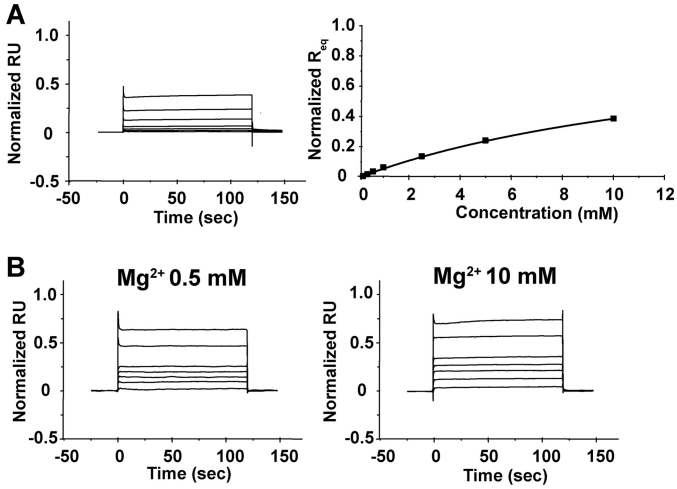

FIGURE 3. **ATP binds to the CBS domains of CNNM2 in a Mg^{2+}-dependent manner.** *A*, sensorgrams showing the binding of Mg^{2+} to immobilized CBS-WT (*left panel*). Mg^{2+} concentration varied from 0.1 to 10 mM (0.1, 0.25, 0.5, 1, 2.5, 5, or 10 mM). Representative data of three independent experiments are shown. *RU*, response unit. Steady-state analyses for binding of Mg^{2+} to CBS-WT surface are also shown (*right panel*). Equilibrium responses (R_{eq}) were plotted as a function of Mg^{2+} concentration and fitted with a 1:1 binding model. *B*, sensorgrams showing the binding of ATP to immobilized CBS-WT in the presence of 0.5 mM Mg^{2+} (*left panel*) or 10 mM Mg^{2+} (*right panel*). ATP concentration varied from 10 to 500 μM (10, 25, 50, 75, 100, 250, or 500 μM). Representative data of three independent experiments are shown.

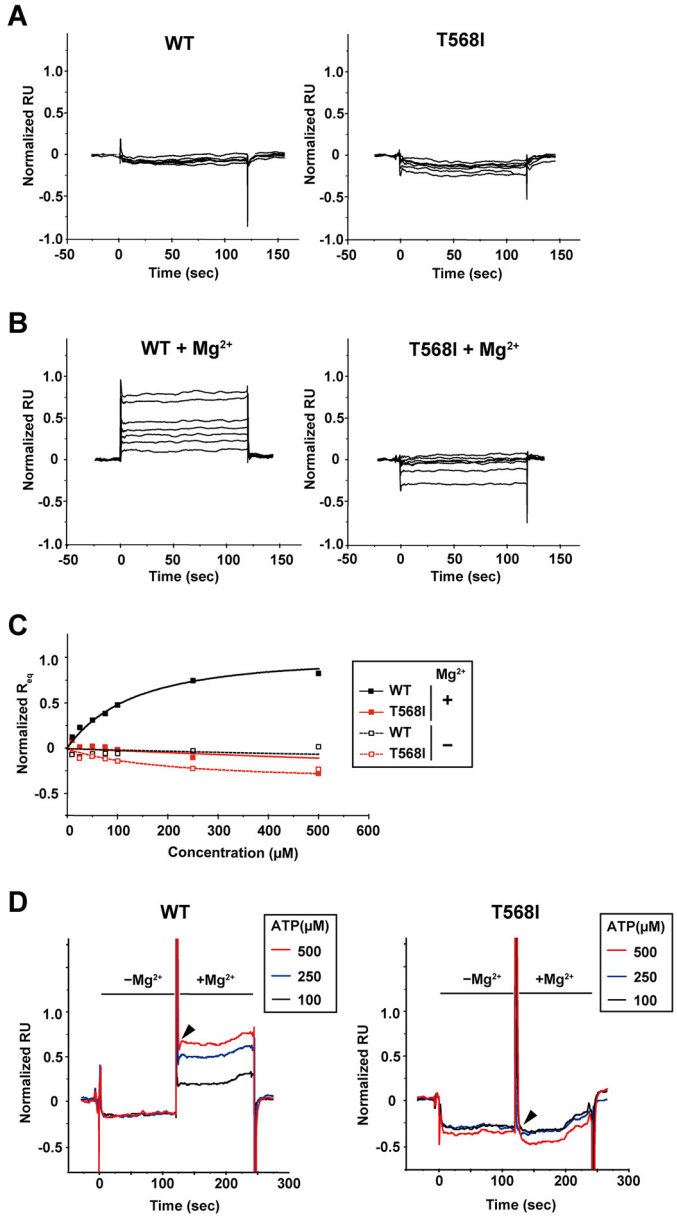

FIGURE 4. **Disease-associated amino acid substitution abrogates the interaction with ATP.** *A* and *B*, sensorgrams showing the binding of ATP to immobilized CBS-WT (*left panel*) or CBS-T568I (*right panel*) in the absence of Mg^{2+} (*A*) or in the presence of 10 mM Mg^{2+} (*B*). ATP concentration varied from 10 to 500 μM for each experiment. Representative data of three independent experiments are shown. *RU*, response unit. *C*, steady-state analysis for binding of ATP to CBS-WT and CBS-T568I surfaces in the presence or absence of 10 mM Mg^{2+}. Equilibrium responses (R_{eq}) extracted from *A* and *B* were plotted as a function of ATP concentration and fitted with a 1:1 binding model. *D*, sensorgrams showing the binding of ATP to immobilized CBS-WT (*left panel*) or CBS-T568I (*right panel*) under the sequential changes of Mg^{2+} concentration. ATP (100, 250, or 500 μM) was injected with a buffer containing no Mg^{2+} for 2 min, and then the buffer was switched to one containing 10 mM Mg^{2+}. The *arrowhead* indicates the time point of the buffer switch. Representative data of three independent experiments are shown.

the responses were similar, indicating that ATP can bind to the CNNM2 CBS domains under both conditions. Thus, we determined to set the concentration of Mg^{2+} in the running buffer as 10 mM in the following experiments. First, we quantitatively compared the ATP binding ability of CBS-WT and CBS-T568I. In the absence of Mg^{2+}, we observed no SPR response (Fig. 4*A*). In the presence of Mg^{2+}, significant and concentration-dependent SPR responses were observed from the CBS-WT surface but not from the CBS-T568I surface (Fig. 4*B*), indicating the occurrence of the Mg^{2+}-dependent interaction between the CNNM2 CBS domains and ATP, which is abolished by the disease-associated mutation. As one adenine nucleotide typically binds to two tandem CBS domains (10), we fitted the steady-state plot of the CBS-WT surface response in the presence of Mg^{2+} to a 1:1 binding model (Fig. 4*C*) and estimated K_d of 141 ± 12 μM (represented as the mean ± S.E. from three independent experiments), which is within the range of those reported for other CBS domains (15).

To further confirm the Mg^{2+} dependence of ATP binding to the CBS domains of CNNM2, we performed SPR analysis with sequential changes of Mg^{2+} concentration in the running buffer. ATP was first injected in the running buffer without Mg^{2+} and then in a buffer containing Mg^{2+}, and changes in SPR responses were observed. As shown in Fig. 4*D*, significant SPR responses were observed with CBS-WT just after the injection of Mg^{2+}, and the amplitude of the responses increased in a manner dependent on the ATP concentration. In contrast, there was no significant SPR response observed from CBS-T568I even after the Mg^{2+} injection. Thus, ATP binding to the CBS domains of CNNM2 requires the presence of Mg^{2+}, indicating that the CBS domains of CNNM2 bind to ATP in a Mg^{2+}-dependent manner.

The Specificity and Uniqueness of ATP Binding to the CBS Domains of CNNM2—To further ascertain the Mg^{2+} dependence of ATP binding to the CBS domains of CNNM2, we performed filter binding assays using [α-^{32}P]ATP as a ligand to detect the amount of ATP bound to proteins trapped on the filter. The results of assays in the presence of 10 mM Mg^{2+} showed a clear saturated binding curve with apparent K_d of 159 ± 28 μM, whereas no binding was observed in the absence of Mg^{2+} (Fig. 5*A* and Table 1). 10 mM Mg^{2+} is much more than the normal cytosolic concentration of Mg^{2+}, and thus, we also performed filter binding assays using the same concentrations of Mg^{2+} as those of ATP. As shown in Fig. 5*A*, CBS-WT showed similar levels of ATP binding signals compared with the experiments using constant 10 mM Mg^{2+}, when the concentrations of ATP and Mg^{2+} were set to 200, 400, and 800 μM, which are far above the reported K_d value between ATP and Mg^{2+} (~78 μM) (28). As most cytosolic ATP forms complexes with Mg^{2+} and the free cytosolic Mg^{2+} level is ~0.5–1 mM, we concluded that the interaction between ATP and CBS-WT is physiological. In contrast, the affinity of CBS-T568I to ATP was significantly lower than that of CBS-WT (Fig. 5*B*), and the estimated K_d value was >1000 μM (Table 1). These data are consistent with the results shown in Fig. 4 and confirm the notion that the CBS domains of CNNM2 bind specifically to ATP in a Mg^{2+}-dependent manner.

The CBS domain is evolutionarily conserved and present in the proteome of archaebacteria, prokaryotes, and eukaryotes, and there are a number of reports stating the binding of CBS domains to ATP (10). However, there have been no reports, to date, showing such clear Mg^{2+} dependence of this interaction as in the case of CNNM2. To examine whether the Mg^{2+}-dependent interaction is a unique feature of the CBS domains of CNNM2, we also performed ATP binding assays using two

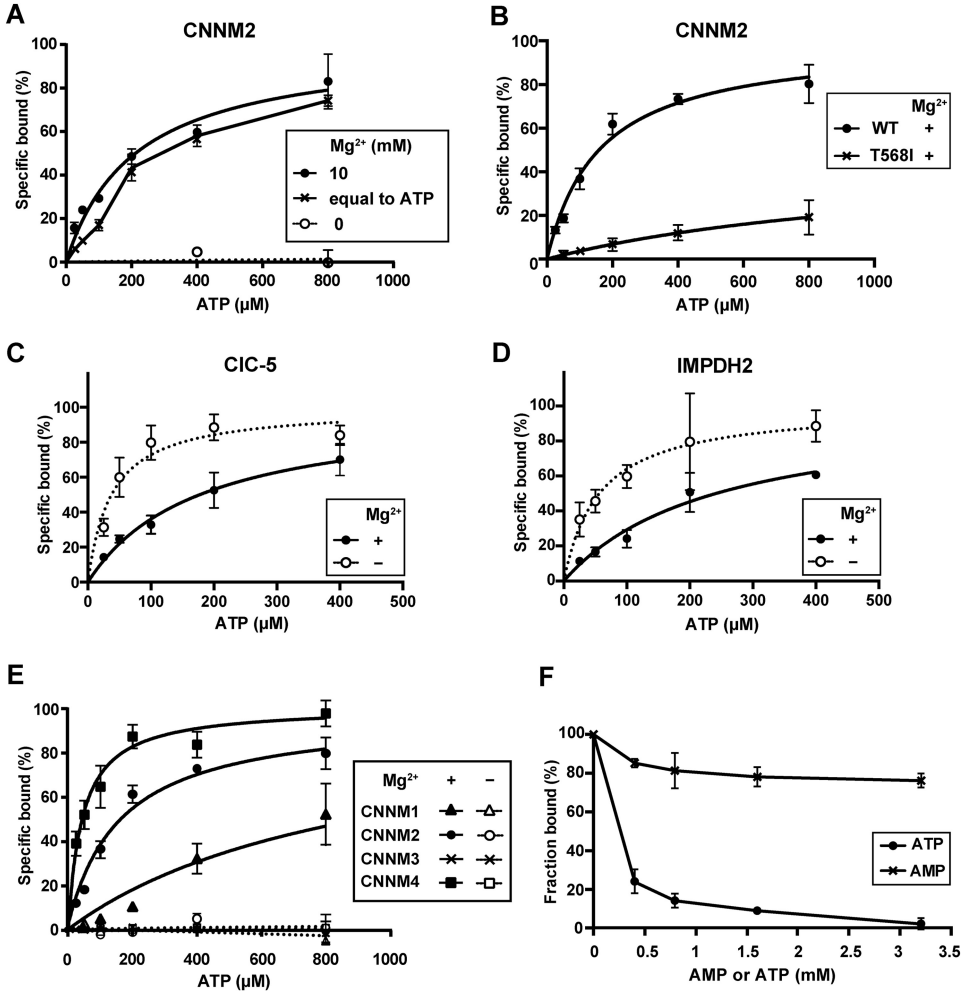

FIGURE 5. **Comparative analyses of the various CBS domains for ATP binding.** *A*, filter binding assays were performed by incubating increasing concentrations of [α-^{32}P]ATP with 50 μM recombinant protein (GST or GST-CBS-WT) in a reaction buffer in the presence of Mg^{2+} at concentrations of 0, 10 mM, or equal to that of ATP for 20 min at 25 °C. Samples were filtered through a nitrocellulose membrane, and the amount of ATP bound to each filter was quantitated by performing liquid scintillation counting. Nonspecific binding was determined by performing control assays with GST and was subtracted. The data were normalized to the percentage of ATP bound at saturation and are represented as the means ± S.E. (*error bars*) of three independent experiments. *B*, filter binding assays using GST-CBS-WT and GST-CBS-T568I in the presence of 10 mM Mg^{2+} were performed as in *A*. *C* and *D*, filter binding assays using the CBS domains of ClC-5 (*C*) and IMPDH2 (*D*) in the presence or absence of 10 mM Mg^{2+} were performed as in *A*. *E*, filter binding assays using the CBS domains of CNNM1–4 in the presence or absence of 10 mM Mg^{2+} were performed as in *A*. *F*, competition assays were performed to examine the binding of GST-CBS-WT to ATP or AMP. ATP or AMP (0.4, 0.8, 1.6, or 3.2 mM) was added to reactions containing 5 μM [α-^{32}P]ATP, 10 mM Mg^{2+}, and GST-CBS-WT, and the assays were performed as in *A*. The data are represented as a percentage of specific binding in the absence of any competitor, and the means ± S.E. (*error bars*) of three independent experiments are shown.

TABLE 1

K_d values obtained from filter binding assays

The K_d values are indicated as the means ± S.E. of three independent measurements.

Protein	ATP		AMP with Mg^{2+}
	With Mg^{2+}	Without Mg^{2+}	
	μM	μM	μM
CNNM2 WT	159 ± 28	No binding	>3200[a]
CNNM2 T568I	>1000	ND[b]	ND
CNNM1	915 ± 389	No binding	ND
CNNM3	No binding	No binding	ND
CNNM4	43.4 ± 8.9	No binding	ND
ClC-5	177 ± 28	37.5 ± 11.3	241 ± 56
IMPDH2	242 ± 78	56.4 ± 7.9	141 ± 58

[a] Estimated from the IC_{50} value obtained from competition assays.
[b] ND, not determined.

other typical CBS domains derived from ClC-5 and IMPDH2, both of which are reported to bind to ATP (15, 19), in the presence or absence of Mg^{2+}. As shown in Fig. 5, *C* and *D*, both ClC-5 and IMPDH2 showed saturable binding with ATP, regardless of the presence or absence of Mg^{2+}. In the presence of Mg^{2+}, K_d values were 177 ± 28 μM for ClC-5 and 242 ± 78 μM for IMPDH2, and in the absence of Mg^{2+}, the K_d values decreased to 37.5 ± 11.3 μM and 56.4 ± 7.9 μM, respectively (Table 1). Therefore, the affinities of the CBS domains of these proteins for ATP were stronger in the absence of Mg^{2+} than in the presence of Mg^{2+}. These results support the notion that Mg^{2+} dependence of the CBS domains of CNNM2 for binding to ATP is a unique feature among the CBS domains. To investigate whether this unique feature is conserved among CNNM family proteins, we also performed filter binding assays using CBS domains derived from CNNM1, CNNM3, and CNNM4. In the presence of Mg^{2+}, all of these proteins, except for CNNM3, showed saturable binding with ATP (Fig. 5*E*). K_d values were 43.4 ± 8.9 μM for CNNM4 and 915 ± 389 μM for CNNM1 (Table 1). Interestingly, these K_d values inversely correlate with the capacities for Mg^{2+} efflux shown in Fig. 1*A*. In

the absence of Mg^{2+}, no binding was observed from all of the proteins (Fig. 5*E*). These results confirm the Mg^{2+} dependence of the interaction of the CNNM CBS domains with ATP and suggest its importance in Mg^{2+} efflux.

In general, CBS domains that bind to ATP can also bind to other adenine nucleotides, such as AMP (15). To examine whether the CBS domains of CNNM2 bind to AMP, we performed filter binding assays using [^{3}H]AMP as a ligand in the presence of Mg^{2+}. Saturable binding curves were obtained from ClC-5 and IMPDH2 with K_d values of 241 ± 56 μM and 141 ± 58 μM, respectively (Table 1), demonstrating their interactions with AMP as reported previously (15, 19). In contrast, AMP binding to CBS-WT of CNNM2 was not saturable, and we could not determine the K_d value (data not shown). Therefore, we performed competition assays using nonradiolabeled ATP or AMP to serve as a competitor against [α-^{32}P]ATP (5 μM). Although nonradiolabeled ATP effectively competed with [α-^{32}P]ATP, even 3.2 mM AMP (the maximum concentration we tested) could only outcompete 24% of [α-^{32}P]ATP, indicating that the IC_{50} value of AMP binding to the CBS domains of CNNM2 is significantly >3.2 mM (Fig. 5*F*). Therefore, AMP does not virtually bind to the CBS domains of CNNM2. Collectively, the interactions between ATP and the CNNM2 CBS domains require the terminal phosphate groups of ATP, which are a unique feature of CNNM2. Because Mg^{2+} is known to form complexes with ATP through interactions with the phosphate groups of ATP, these results suggest that Mg-ATP is the true ligand for the CNNM2 CBS domains.

Electronegative Potentials around the ATP Binding Site of the CBS Domains of CNNMs—There are several examples of proteins that require Mg^{2+} to bind to ATP. In the cases of sarcoplasmic reticulum Ca^{2+}-ATPase and 6-hydroxymethyl-7,8-dihydropterin pyrophosphokinase (26, 27), Mg^{2+} neutralizes the electrostatic repulsion force between the electronegative surface potentials around the ATP binding site and negatively charged phosphate groups of ATP. Therefore, we compared the electrostatic surface potentials of the ATP binding sites between CNNM2, ClC-5, and IMPDH2. The electrostatic surface potentials were calculated for homology models of the CBS domains of CNNM2 and IMPDH2 based on the crystal structures of their bacterial homologs (21) and the previously solved crystal structure of the CBS domains of ClC-5 in complex with ATP (19). As shown in Fig. 6*A*, CNNM2 showed highly electronegative surface potentials around the ATP binding site, whereas both ClC-5 and IMPDH2 showed highly electropositive surface potentials, which would be suitable for the electrostatic interactions with the phosphate groups of ATP. This clear difference in the surface potentials presumably explains the unique requirement of Mg^{2+} for the interactions between ATP and the CNNM2 CBS domains. We also calculated the electrostatic surface potentials for homology models of the CBS domains of CNNM1 and CNNM4. As shown in Fig. 6*B*, both CNNM1 and CNNM4 showed similar electronegative potentials around the ATP binding site as did CNNM2, which is consistent with their unique requirement of Mg^{2+} for the interactions with ATP.

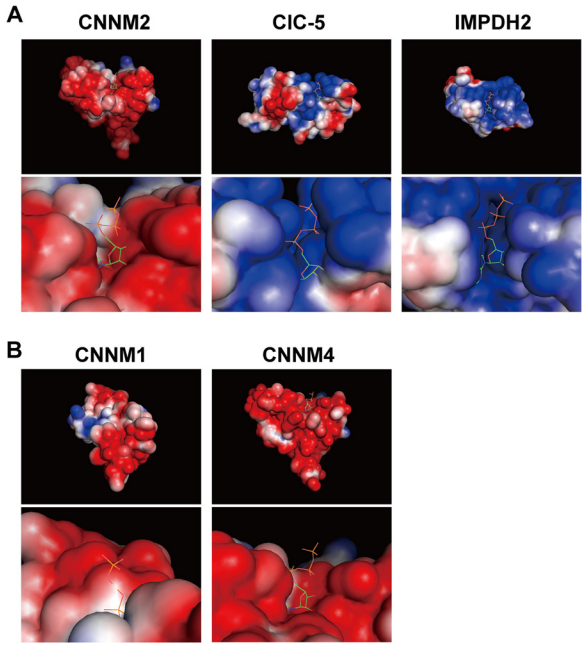

FIGURE 6. **Comparison of electrostatic surface potential maps of the ATP binding sites.** *A*, the electrostatic surface potential maps of the entire CBS domains (*upper*) and magnified images around the ATP binding site (*lower*) are visualized with *colors* ranging from *blue* to *red* (from +2 kT/e to −2 kT/e). ATP is represented as *sticks* in atomic coloring (*blue*, nitrogen; *green*, carbon; *orange*, phosphorus; and *red*, oxygen). To calculate electrostatic surface potentials, the following structures of CBS domains in complex with ATP were used: a homology model based on the crystal structure of CorC from *B. parapertussis* (PDB ID 3JTF) for CNNM2, the crystal structure of human ClC-5 (PDB ID 2J9L) for ClC-5, and a homology model based on the crystal structure of IMPDH from *P. aeruginosa* (PDB ID 4DQW) for IMPDH2. *B*, the electrostatic surface potential maps of the entire CBS domains (*upper*) and magnified images around the ATP binding site (*lower*) of CNNM1 and CNNM4 were created and visualized as CNNM2 in *A*.

DISCUSSION

In this study, we have shown that the CBS domains of CNNM2 bind to ATP in a Mg^{2+}-dependent manner, which presumably contributes to the Mg^{2+} efflux function of CNNM2. The possibility of ATP binding to the CBS domains of CNNM2 was theoretically predicted in a previous report by using a homology model, which was based on the structural data of *B. parapertussis* CorC (29). In this model, the evolutionary conserved threonine (Thr-568) is located at the region predicted to form the ATP binding pocket and also forms a hydrogen bond that stabilizes the position of the Glu-570 and Asp-571 residues. The substitution of Thr-568 into the bigger isoleucine residue was predicted to cause steric bumps with the ATP molecule and also alter the position of the Glu-570 and Asp-571 residues. Therefore, the substitution was proposed to severely affect ATP binding. In this study, we confirmed these predictions experimentally by performing binding analyses; ATP was determined to bind to the CBS domains of CNNM2, and this binding was abrogated by T568I mutation. Moreover, we further demonstrated the Mg^{2+} dependence of this binding, which was not accounted for in the predicted model. To the best of our knowledge, Mg^{2+} dependence for binding to ATP has never been reported to occur in other CBS domains. Comparative analyses of electrostatic surface potentials of the CBS domains revealed the presence of highly electronegative potentials around the ATP binding site of the CBS domains of CNNM2,

which may explain the unique requirement of Mg^{2+} in the case of CNNM2.

So far, the biochemical importance of the interaction between CNNM2 and ATP remains unknown. Notably, AMPK binds to AMP or ADP with higher affinity than that of ATP (in the presence of Mg^{2+}, similar to the physiological condition) and is regulated in response to changes in the intracellular AMP/ATP or ADP/ATP ratio, enabling AMPK to respond dynamically to the energetic state of cells (17, 18). Thus, the CBS domains of AMPK are believed to function as a cellular energy sensor (30, 31). However, in the case of CNNM2, the CBS domains have a unique feature such that they selectively bind to ATP with a relatively low K_d of ~150 μM, which is considerably lower than the ATP concentrations typically found in cells (1–10 mM) (32), and virtually does not bind to AMP. Therefore, the CBS domains of CNNM2 are considered to constitutively bind to ATP irrespective of the energetic state of cells. Another unique feature of the CBS domains of CNNM2 is the strict Mg^{2+} dependence of its binding ability to ATP. In mammalian cells, the majority of intracellular Mg^{2+} is present in the form of complexes with various intracellular molecules, such as phospholipids, proteins, and nucleic acids (28, 33). Among these Mg^{2+}-binding biomolecules, ATP represents a major component because of its abundance (1–10 mM) and relatively high Mg^{2+} binding affinity (K_d of ~78 μM); hence, most ATP is considered to exist as Mg-ATP within the cells (28). Taking this into account, we hypothesize that the CBS domains of CNNM2 may utilize their ATP binding ability for efficiently recruiting Mg^{2+}. Indeed, intracellular Mg-ATP (1–10 mM) is much more abundant than free Mg^{2+} (0.5–1 mM) (28), and the size of Mg-ATP is much larger than that of Mg^{2+}, which would be beneficial for molecular recognition. Once Mg^{2+} is dissociated from Mg-ATP, it is supplied as a substrate for efflux, and Mg^{2+}-free ATP dissociates from the CBS domains due to the loss of affinity. Then, another Mg-ATP can immediately occupy the binding site. Repeating this sequential process, Mg^{2+} can be efficiently supplied to facilitate Mg^{2+} efflux via CNNM2. This hypothesis should be tested in the future by much more detailed studies, such as structural analyses.

The T568I mutation of CNNM2 associated with human hereditary hypomagnesemia abrogated not only its ATP binding ability but also its Mg^{2+} efflux function, suggesting the physiological importance of Mg^{2+} efflux by CNNM2 in the regulation of magnesium homeostasis at the organismal level. In a previous study, we showed that CNNM4 localizes to the basolateral membrane of intestinal epithelial cells and mediates transcellular Mg^{2+} transport across epithelia by extruding intracellular Mg^{2+} to the outside of cells (7). In addition, *CNNM4*-knock-out mice exhibited mild hypomagnesemia due to the intestinal malabsorption of magnesium. Considering these similarities between CNNM2 and CNNM4, we speculate that CNNM2 also mediates transcellular Mg^{2+} transport across epithelia, like CNNM4 does. In support of this possibility, two previous papers have reported a strong expression and localization of CNNM2 at the basolateral membrane of distal convoluted tubule cells in the kidney (6, 29), where renal reabsorption of magnesium by transcellular Mg^{2+} transport is known to occur. CNNM2 presumably plays an important role in the renal reabsorption of magnesium by promoting Mg^{2+} efflux from the distal convoluted tubule cells to the inner parts of the body, which should be the focus of future studies on CNNM2.

Acknowledgments—We thank Dr. R. Dutzler for providing the cDNA encoding the CBS domains of ClC-5 inserted in the pET28 b+ plasmid; Drs. I. Nishina, T. Sangawa, Y. Kitago, J. Takagi, and H. Nakamura for technical advice in the ATP-protein interaction analyses; and H. Yamamoto, M. Matsuda, and A. Kawasaki for skillful technical assistance.

REFERENCES

1. Alexander, R. T., Hoenderop, J. G., and Bindels, R. J. (2008) Molecular determinants of magnesium homeostasis: insights from human disease. *J. Am. Soc. Nephrol.* **19,** 1451–1458
2. Quamme, G. A. (2010) Molecular identification of ancient and modern mammalian magnesium transporters. *Am. J. Physiol. Cell Physiol.* **298,** C407–429
3. Wang, C. Y., Shi, J. D., Yang, P., Kumar, P. G., Li, Q. Z., Run, Q. G., Su, Y. C., Scott, H. S., Kao, K. J., and She, J. X. (2003) Molecular cloning and characterization of a novel gene family of four ancient conserved domain proteins (ACDP). *Gene* **306,** 37–44
4. Gibson, M. M., Bagga, D. A., Miller, C. G., and Maguire, M. E. (1991) Magnesium transport in *Salmonella typhimurium*: the influence of new mutations conferring Co^{2+} resistance on the CorA Mg^{2+} transport system. *Mol. Microbiol.* **5,** 2753–2762
5. Goytain, A., and Quamme, G. A. (2005) Functional characterization of ACDP2 (ancient conserved domain protein), a divalent metal transporter. *Physiol. Genomics* **22,** 382–389
6. Stuiver, M., Lainez, S., Will, C., Terryn, S., Günzel, D., Debaix, H., Sommer, K., Kopplin, K., Thumfart, J., Kampik, N. B., Querfeld, U., Willnow, T. E., Němec, V., Wagner, C. A., Hoenderop, J. G., Devuyst, O., Knoers, N. V., Bindels, R. J., Meij, I. C., and Müller, D. (2011) *CNNM2*, encoding a basolateral protein required for renal Mg^{2+} handling, is mutated in dominant hypomagnesemia. *Am. J. Hum. Genet.* **88,** 333–343
7. Yamazaki, D., Funato, Y., Miura, J., Sato, S., Toyosawa, S., Furutani, K., Kurachi, Y., Omori, Y., Furukawa, T., Tsuda, T., Kuwabata, S., Mizukami, S., Kikuchi, K., and Miki, H. (2013) Basolateral Mg^{2+} extrusion via CNNM4 mediates transcellular Mg^{2+} transport across epithelia: a mouse model. *PLoS Genet.* **9,** e1003983
8. Polok, B., Escher, P., Ambresin, A., Chouery, E., Bolay, S., Meunier, I., Nan, F., Hamel, C., Munier, F. L., Thilo, B., Mégarbané, A., and Schorderet, D. F. (2009) Mutations in *CNNM4* cause recessive cone-rod dystrophy with amelogenesis imperfecta. *Am. J. Hum. Genet.* **84,** 259–265
9. Parry, D. A., Mighell, A. J., El-Sayed, W., Shore, R. C., Jalili, I. K., Dollfus, H., Bloch-Zupan, A., Carlos, R., Carr, I. M., Downey, L. M., Blain, K. M., Mansfield, D. C., Shahrabi, M., Heidari, M., Aref, P., Abbasi, M., Michaelides, M., Moore, A. T., Kirkham, J., and Inglehearn, C. F. (2009) Mutations in *CNNM4* cause Jalili syndrome, consisting of autosomal-recessive cone-rod dystrophy and amelogenesis imperfecta. *Am. J. Hum. Genet.* **84,** 266–273
10. Baykov, A. A., Tuominen, H. K., and Lahti, R. (2011) The CBS domain: a protein module with an emerging prominent role in regulation. *ACS Chem. Biol.* **6,** 1156–1163
11. Bateman, A. (1997) The structure of a domain common to archaebacteria and the homocystinuria disease protein. *Trends Biochem. Sci.* **22,** 12–13
12. Hattori, M., Tanaka, Y., Fukai, S., Ishitani, R., and Nureki, O. (2007) Crystal structure of the MgtE Mg^{2+} transporter. *Nature* **448,** 1072–1075
13. Hattori, M., Iwase, N., Furuya, N., Tanaka, Y., Tsukazaki, T., Ishitani, R., Maguire, M. E., Ito, K., Maturana, A., and Nureki, O. (2009) Mg^{2+}-dependent gating of bacterial MgtE channel underlies Mg^{2+} homeostasis. *EMBO J.* **28,** 3602–3612
14. Ignoul, S., and Eggermont, J. (2005) CBS domains: structure, function, and

pathology in human proteins. *Am. J. Physiol. Cell Physiol.* **289,** C1369–1378
15. Scott, J. W., Hawley, S. A., Green, K. A., Anis, M., Stewart, G., Scullion, G. A., Norman, D. G., and Hardie, D. G. (2004) CBS domains form energy-sensing modules whose binding of adenosine ligands is disrupted by disease mutations. *J. Clin. Invest.* **113,** 274–284
16. Xiao, B., Heath, R., Saiu, P., Leiper, F. C., Leone, P., Jing, C., Walker, P. A., Haire, L., Eccleston, J. F., Davis, C. T., Martin, S. R., Carling, D., and Gamblin, S. J. (2007) Structural basis for AMP binding to mammalian AMP-activated protein kinase. *Nature* **449,** 496–500
17. Xiao, B., Sanders, M. J., Underwood, E., Heath, R., Mayer, F. V., Carmena, D., Jing, C., Walker, P. A., Eccleston, J. F., Haire, L. F., Saiu, P., Howell, S. A., Aasland, R., Martin, S. R., Carling, D., and Gamblin, S. J. (2011) Structure of mammalian AMPK and its regulation by ADP. *Nature* **472,** 230–233
18. Oakhill, J. S., Steel, R., Chen, Z. P., Scott, J. W., Ling, N., Tam, S., and Kemp, B. E. (2011) AMPK is a direct adenylate charge-regulated protein kinase. *Science* **332,** 1433–1435
19. Meyer, S., Savaresi, S., Forster, I. C., and Dutzler, R. (2007) Nucleotide recognition by the cytoplasmic domain of the human chloride transporter ClC-5. *Nat. Struct. Mol. Biol.* **14,** 60–67
20. Lis, M., Kim, T., Sarmiento, J. J., Kuroda, D., Dinh, H. V., Kinjo, A. R., Amada, K., Devadas, S., Nakamura, H., and Standley, D. M. (2011) Bridging the gap between single-template and fragment based protein structure modeling using Spanner. *Immunome Res.* **7,** 1–8
21. Labesse, G., Alexandre, T., Vaupré, L., Salard-Arnaud, I., Him, J. L., Raynal, B., Bron, P., and Munier-Lehmann, H. (2013) MgATP regulates allostery and fiber formation in IMPDHs. *Structure* **21,** 975–985
22. Kinjo, A. R., and Nakamura, H. (2007) Similarity search for local protein structures at atomic resolution by exploiting a database management system. *BIOPHYSICS* **3,** 75–84
23. Baker, N. A., Sept, D., Joseph, S., Holst, M. J., and McCammon, J. A. (2001) Electrostatics of nanosystems: application to microtubules and the ribosome. *Proc. Natl. Acad. Sci. U.S.A.* **98,** 10037–10041
24. Cai, J., Daoud, R., Alqawi, O., Georges, E., Pelletier, J., and Gros, P. (2002) Nucleotide binding and nucleotide hydrolysis properties of the ABC transporter MRP6 (ABCC6). *Biochemistry* **41,** 8058–8067
25. Tameling, W. I., Elzinga, S. D., Darmin, P. S., Vossen, J. H., Takken, F. L., Haring, M. A., and Cornelissen, B. J. (2002) The tomato R gene products I-2 and MI-1 are functional ATP binding proteins with ATPase activity. *Plant Cell* **14,** 2929–2939
26. Blaszczyk, J., Shi, G., Yan, H., and Ji, X. (2000) Catalytic center assembly of HPPK as revealed by the crystal structure of a ternary complex at 1.25 Å resolution. *Structure* **8,** 1049–1058
27. McIntosh, D. B., Clausen, J. D., Woolley, D. G., MacLennan, D. H., Vilsen, B., and Andersen, J. P. (2004) Roles of conserved P domain residues and Mg^{2+} in ATP binding in the ground and Ca^{2+}-activated states of sarcoplasmic reticulum Ca^{2+}-ATPase. *J. Biol. Chem.* **279,** 32515–32523
28. Romani, A. M. (2011) Cellular magnesium homeostasis. *Arch. Biochem. Biophys.* **512,** 1–23
29. de Baaij, J. H., Stuiver, M., Meij, I. C., Lainez, S., Kopplin, K., Venselaar, H., Müller, D., Bindels, R. J., and Hoenderop, J. G. (2012) Membrane topology and intracellular processing of cyclin M2 (CNNM2). *J. Biol. Chem.* **287,** 13644–13655
30. Kahn, B. B., Alquier, T., Carling, D., and Hardie, D. G. (2005) AMP-activated protein kinase: ancient energy gauge provides clues to modern understanding of metabolism. *Cell Metab.* **1,** 15–25
31. Carling, D., Mayer, F. V., Sanders, M. J., and Gamblin, S. J. (2011) AMP-activated protein kinase: nature's energy sensor. *Nat. Chem. Biol.* **7,** 512–518
32. Beis, I., and Newsholme, E. A. (1975) The contents of adenine nucleotides, phosphagens and some glycolytic intermediates in resting muscles from vertebrates and invertebrates. *Biochem. J.* **152,** 23–32
33. Günther, T. (2006) Concentration, compartmentation and metabolic function of intracellular free Mg^{2+}. *Magnes. Res.* **19,** 225–236